Light-Dark Cycle Memory in the Mammalian Suprachiasmatic Nucleus

Mark C. Ospeck,[†*] Ben Coffey,[†] and Dave Freeman[‡]
[†]Physics Department and [‡]Biology Department, University of Memphis, Memphis, Tennessee

ABSTRACT The mammalian circadian oscillator, or suprachiasmatic nucleus (SCN), contains several thousand clock neurons in its ventrolateral division, many of which are spontaneous oscillators with period lengths that range from 22 to 28 h. In complete darkness, this network synchronizes through the exchange of action potentials that release vasoactive intestinal polypeptide, striking a compromise, free-running period close to 24 h long. We entrained Siberian hamsters to various light-dark cycles and then tracked their activity into constant darkness to show that they retain a memory of the previous light-dark cycle before returning to their own free-running period. Employing Leloup-Goldbeter mammalian clock neurons we model the ventrolateral SCN network and show that light acting weakly upon a strongly rhythmic vasoactive intestinal polypeptide oscillation can explain the observed light-dark cycle memory. In addition, light is known to initiate a mitogen-activated protein kinase signaling cascade that induces transcription of both *per* and *mkp1* phosphatase. We show that the ensuing phosphatase-kinase interaction can account for the dead zone in the mammalian phase response curve and hypothesize that the SCN behaves like a lock-in amplifier to entrain to the light edges of the circadian day.

INTRODUCTION

Mammals have two suprachiasmatic nuclei (SCN), one per hemisphere, located in the hypothalamus just above the optic chiasm. These two neural networks constitute the mammalian circadian clock, the master clock responsible for driving circadian locomotor activity rhythms and synchronizing these rhythms to the 24-h day. Within the SCN, clock neurons are synaptically coupled so that they synchronize their biochemical limit cycles together in complete darkness (1,2,3). Mammals exhibit multiple circadian rhythms in physiology and behavior that persist in constant conditions and exhibit a coherent period length in the absence of external time cues (4), with the SCN being the principal coordinator of these rhythms (5).

Rhythmic activity of SCN neurons is thought to be driven by the rhythmic expression of so-called clock genes (*per*1, *per*2, *per*3, *cry*1, *cry*2, *bmal*1, and *reverbα*) and individual neurons exhibit circadian rhythms in electrical activity and gene expression in vitro that have independent period lengths and phases (6). However, for synchronization to occur between clock neurons, intercellular interaction appears to be necessary, because SCN neurons placed at low densities in culture exhibit rhythmic activity, but fail to synchronize together (6). Also, exposing SCN neurons to tetrodotoxin in vitro causes desynchronization, which suggests that synaptic communication is involved in their synchronization (3,7). In support of this hypothesis, synchrony is observed in SCN slices or SCN neurons kept in vitro at high densities, which presumably allows synaptic communication between them (3,7).

Neuropeptides, including vasoactive intestinal polypeptide (VIP (3,8)) and gastrin-releasing peptide (9), together with the neurotransmitter gamma aminobutyric acid (GABA (10)), have been considered as synchronization factors in the SCN. Recent results support an integral role for VIP in both intracellular timekeeping and intercellular synchrony among SCN neurons (3,8,11). Synchrony among neurons is lost in knockout mice lacking VIP ($VIP^{-/-}$) or its receptor $VPAC_2$, which is a product of the *Vipr*2 gene (8). Treatment of $VIP^{-/-}$ mice with a $VPAC_2$ agonist restored rhythmicity and synchrony in cultured SCN neurons (8). Also, exposure to exogenous VIP resulted in phase shifts of individual SCN neurons, as well as phase shifts at the behavioral level (12,13). Increases in $VPAC_2$ receptor number caused more rapid reentrainment to phase shifts of the light-dark cycle in mice and desynchronized their rhythms in constant darkness (14). In addition, mice that lacked the $VPAC_2$ receptor exhibited arrhythmic activity in constant darkness (15). Both VIP and the $VPAC_2$ receptor appear to be essential for circadian function in the mouse SCN (15).

The neurotransmitter GABA exhibits a circadian rhythm of release in the SCN (16) and exogenously applied GABA phase-shifts the neuronal firing rate of SCN neurons in vitro, whereas daily administration of GABA synchronizes this rhythm (10). Ionotropic $GABA_A$, as well as the G-protein-coupled $GABA_B$ receptors, is expressed within the SCN (3), and there is evidence that GABA contributes to synchrony, although in a less direct way than does VIP (17).

Previous models of the SCN investigated its synchronization through the nonuniform oscillator equation (18), via synthetic genetic circuits called repressilators (19), by using gate cells to couple van der Pol oscillators together (20), and by a mean field coupling of the neuropeptide VIP between biophysics-based models of clock neurons (21–23). Meanwhile, individual mammalian clock neuron biochemistry has been extensively modeled (24,25–27), along with a detailed model of VIP activating the $VPAC_2$ receptor,

Submitted December 23, 2008, and accepted for publication June 8, 2009.

*Correspondence: mospeck@memphis.edu

Editor: Arthur Sherman.

0006-3495/09/09/1513/12 $2.00

doi: 10.1016/j.bpj.2009.06.010

causing activation of a cyclic adenosine monophosphate (cAMP)/protein kinase A (PKA) intercellular signaling pathway (28). Recently, there has been a great deal of interest in biophysics-based models over qualitative modeling (29) and also in heterogeneous modeling of the SCN (30).

We show experimentally that the Siberian hamster (*Phodopus sungorus*), a nocturnal mammal, forms a memory for the particular light-dark cycle to which it was entrained. We then use Leloup-Goldbeter model mammalian clock neurons (24) to make a biophysics-based model of the ventrolateral (VL) subdivision of the SCN to try to account for the light-dark cycle memory we observe.

METHODS

Animals were cared for in accordance with the University of Memphis Institutional Animal Care and Use Committee. Siberian hamsters were placed one per cage, each with a running wheel wired to make one spike per wheel revolution. Running wheel "actograms" were then acquired by Clocklab data analysis and collection software (Coulbourn Instruments, Allentown, PA), which ran on a PC running a Windows XP operating system. Activity was continuously recorded first with the animals placed on various light-dark schedules for a number of weeks and afterward with the animals in constant darkness for several weeks. We employed light-dark schedules that usually involved phase-advancing the lights-off time by 5–20 min/day. Clocklab software was used to turn on and off two 11-W incandescent bulbs. For certain static light-dark schedules such as 10–14 light-dark fluorescent room lights were used. The four fluorescent lights were expected to provide ~11,000 Lumens of flux and actually gave ~2000 candles/m^2 when measured by using a spot meter at the animal cages, similar to the incandescent lamps. Actograms were then analyzed using Clocklab software, which made linear fits to the onset of running wheel activity. These fits were used to determine the circadian period of the animal when it was entrained to a given cycle and the circadian period for the first several days in the constant darkness that followed a particular light-dark cycle. Also, we obtained the animal's free-running period by making fits after the animal had spent several weeks in constant darkness.

EXPERIMENTAL RESULTS

A series of running-wheel activity experiments were performed on Siberian hamsters to study the memory they would retain of a particular light-dark cycle when the cycle was immediately followed by a period of constant darkness. Fig. 1, *A–D*, shows actograms for animals that were entrained to static 10–14, 14–10, 11–11, and 13–13 light-dark cycles. Animals were first entrained to a particular light-dark cycle, and this was followed by constant darkness. A linear best fit to the animal's onset of activity was made when it was entrained to the cycle and also for the next several days in constant darkness. To quantify the number of days of cycle memory, we examined the standard deviation for the best fit to activity onset as a function of the number of days in constant darkness. Animals entrained to cycles with a 24-h period length usually persisted with several days of memory for that cycle ($n = 22$, average cycle memory $= 2.0 \pm 0.3$ days). We performed a p-test using the null hypothesis that these animals had no memory, obtaining $p \sim 10^{-7}$, which led us to conclude that Siberian hamsters retain a significant amount of memory for a light-dark cycle whose period length was close to 24 h. We note that the average free-running period for 31 animals was 23.8 ± 0.4 h. Next, we tested a second group of animals on light-dark cycles either longer or shorter than 24 h by a couple of hours (11–11 h, and 13–13 h). Here, the animals retained on average <1 day of memory ($n = 9$, average cycle memory $= 0.8 \pm 0.15$ days, $p \sim 0.0004$ for no-memory null hypothesis). Thus, the second group also showed a small amount of memory. We also did a preliminary range of entrainment experiments on a small number of Siberian hamsters and found that 2 of 4 animals were able to entrain to a 10-10 cycle, 3 of 12 were able to entrain to an 11-11 cycle, and 6 of 12 were able to entrain to a 13-13 cycle, but 0 of 4 were able to entrain to a 14-14 cycle. Twenty-six results were discarded, due in almost all cases to the animal's failure to properly entrain to the light schedule. Fig. 1, *E–H*, shows that a nocturnal mammal also clearly retains several days of memory for the position of a slowly moving light-dark edge. Typically, we would start the animals on a 16-8 cycle and then phase-advance their lights-off time by 5–20 min/day, trading hours of light for hours of darkness while maintaining a 24-h period. We intended that these changes would mimic the changes in day length occurring at high latitudes near an equinox.

Evidently, Siberian hamsters are able to form a short-term memory of the particular light-dark cycle to which they are entrained and are also able to anticipate slowly changing light-dark cycles. We chose to focus on the light-dark edge and activity onset because nocturnal animals normally start their activity at lights-off and light is thought to be the primary zeitgeiber, or time giver, in the SCN (1,2). Since synaptic input from the retina is made to the VL part of the SCN, which is thought to be principally responsible for synchronization of the entire organ (3,7,31), in modeling it, we try to account for synchronization and light-dark cycle memory.

Model

Different regions of the SCN employ different neuropeptide transmitters, and there is evidence that these regions are distinct oscillators (32). Action potentials from neurons in the VL part of the SCN transmit VIP. Leloup and Goldbeter (LG) (24) have constructed a low-dimensional model of a mammalian clock neuron, and we couple these neurons via action potentials that exchange VIP to model the VL SCN. The LG model neuron contains three circadian biochemical feedback loops. Its repressor loop uses the clock proteins PER and CRY in an ~12-h negative feedback loop in which *per* and *cry* RNAs are first transcribed and then translated into proteins that dimerize (Fig. 2 *A*). Subsequently, PER-CRY protein dimers enter the nucleus to repress both *per* and *cry* RNA transcription by binding to the CLOCK-BMAL1 dimers that promote such transcription. Note that a 12-h negative feedback loop means that

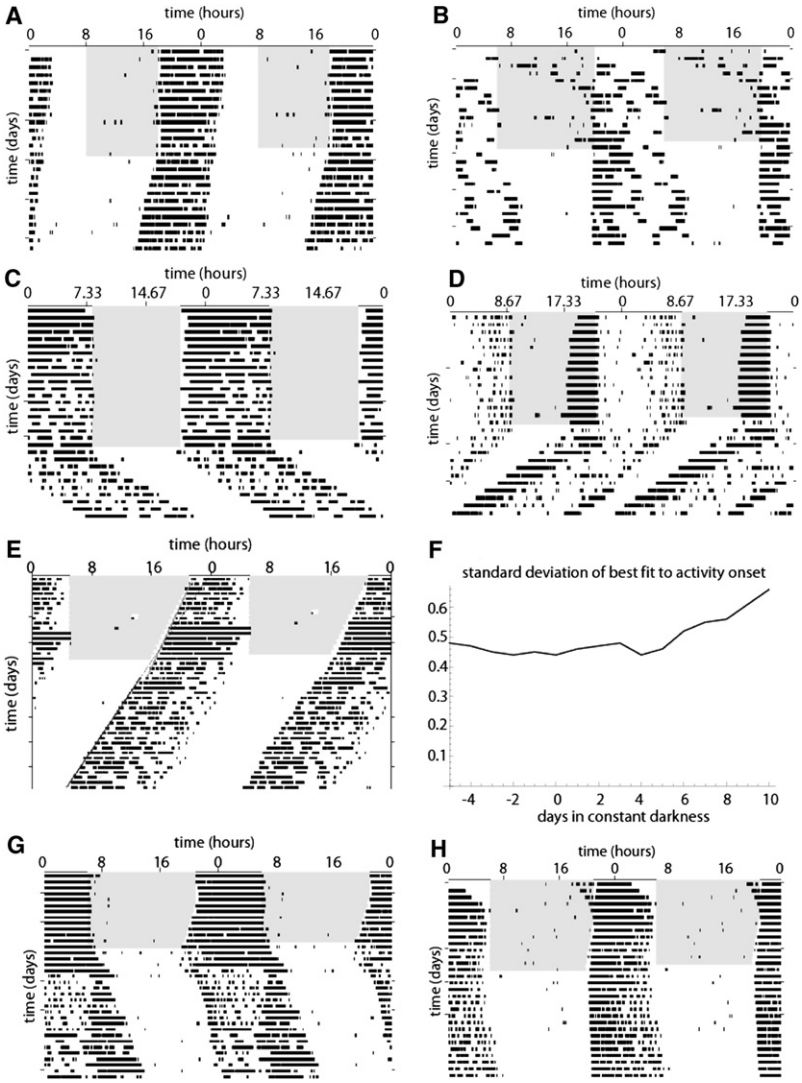

FIGURE 1 Siberian hamsters form a memory for the particular light-dark cycle to which they are entrained. Shown are running-wheel actograms for these nocturnal mammals, whose activity normally starts at lights off. The actogram is repeated with pairs of days plotted side by side. Black bars indicate running-wheel activity; the gray region shows the duration of the light period as the day number increases from top to bottom. The animal is first entrained to a particular cycle, which is followed by constant darkness. Linear least-square fits to activity onset are used to quantify the number of days of memory an animal retains for a particular cycle. (*A*) Entrainment to a 10-14 light-dark cycle followed by ~2 days of memory. (*B*) Entrainment to a 14-10 cycle followed by ~2 days of memory. (*C*) Entrainment to an 11-11 cycle followed by 1 day of memory. (*D*) Entrainment to a 13-13 cycle followed by 1 day of memory. Note here that activity onset precedes the light-dark edge by a large phase angle. Siberian hamsters also form a memory for the rate of change of a particular light-dark cycle to which they are entrained. Two fits are shown: first, a linear fit to the animal's onset of activity when it is entrained to the cycle and for the next several days in constant darkness; and, well into constant darkness, a fit made to determine the animal's FRP. (*E*) Animal with a short FRP (23.58 h) starts on a 16-8 cycle where lights-off is phase-advanced by 20 min/day for 15 days. Afterward, in constant darkness, the animal retains ~4 days of memory for the phase-advancing dark edge. (*F*) Standard deviation for the best fit to activity onset in *E* begins to increase after ~5 days in constant darkness are included in the fit. (*G*) An animal with a long (24.19-h) FRP retains ~3 days of memory for the phase-advancing light-dark cycle, from a 16-8 cycle where lights-off was phase-advanced by 15 min/day for 7 days. (*H*) Animal with a 24.05-h FRP is started on a 16-8 cycle where lights-off is phase-advanced by 10 min/day for 7 days. The animal retains ~2 days of memory for this phase-advancing cycle.

input of a pulse of *per* RNA results in a negative response in *per* RNA in 12 h. A second promoter feedback loop is also an ~12-h negative feedback loop in which nuclear BMAL1 represses its own transcription. Also, there is a REVERBα negative feedback loop in which CLOCK-BMAL1 induces *reverb*α transcription, with REVERBα protein later relocating to the nucleus to repress *bmal1* transcription. This REVERBα loop is one of several interesting lithium-sensitive components of the clock (33–35); however, it is not part of the LG basic model, so to keep things as simple as possible we do not include it here.

However, there is clear experimental evidence that constant light lowers the content of VIP within the SCN, exponentially damping it with an ~8-h time constant (36). Consistent with this, the VIP content of the SCN oscillates in a circadian fashion when locked to a 12-12 light-dark cycle and exhibits a smaller, but similar, oscillation in constant darkness (36). During daylight or subjective day, when firing rate and VIP exchange is high, SCN VIP content continues to decrease. This leads us to include a third ~12-h negative feedback loop in which the VIP received by a clock neuron slowly damps that neuron's own VIP production. The neuropeptide VIP is a rhythmically expressed clock protein that meets most of the criteria for being a synchronizing factor (3), and neuropeptides are transcribed so that they offer a natural mechanism for coupling between biochemistry and electrical firing activity within a network of neurons. VIP has many effects. Specifically, it is known to induce transcription of *per* (37) and *mkp1* (38), a phosphatase for MAP kinase. In addition, it depolarizes a clock neuron by ~12 mV and initiates a subthreshold membrane potential oscillation, both of which act to increase firing rate (16, 40–42).

Expression of the clock gene *per* is induced by light. In constant darkness, *per* RNA is known to peak around time circadian time 8 during the subjective day while 15-min light pulses act to sharply increase *per* RNA levels within ~1 h (37). Light striking retinal ganglion cells causes cotransmission of both pituitary-adenylate-cyclase-activating polypeptide (PACAP) and glutamate along axons of the retinohypothalamic

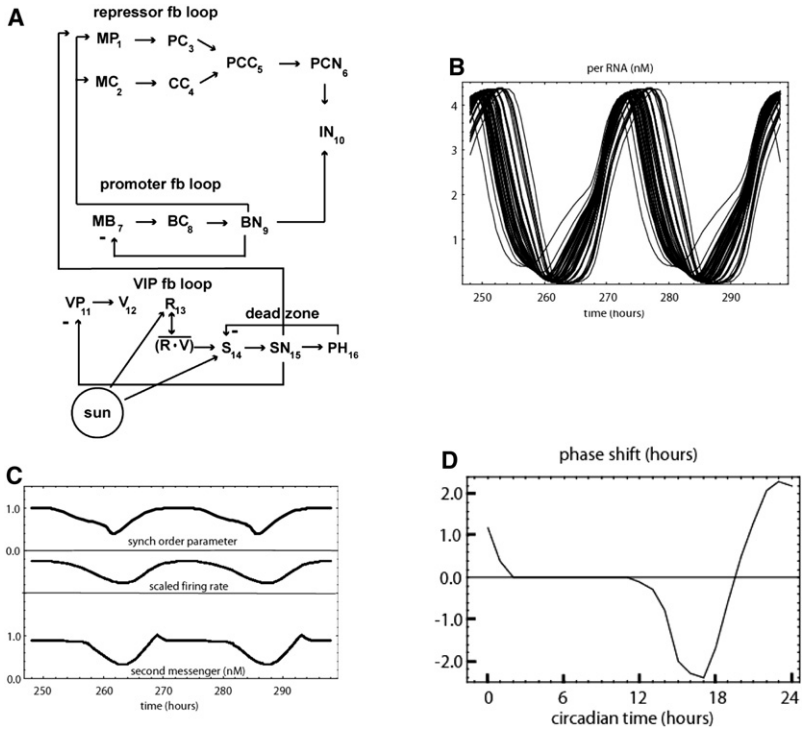

FIGURE 2 (*A*) Sixteen dynamical variables and four feedback loops represent each clock neuron. Indices show the corresponding equation number in the Appendix. In constant darkness, an oscillation in the neuropeptide VIP (*V*) drives oscillations in the firing rate (*R*), which peaks near CT7, and in the second messenger (*S*), which causes *per* RNA (*MP*) to peak near CT8, synchronizing the network (37,44). All feedback loops are internal within a single clock neuron, except that in the VIP loop it is the average rate of receiving VIP from other clock neurons $\overline{(R \times V)}$ that sets the target firing rate and second messenger. Light acts in this loop to increase the firing rate and second messenger, causing induction of *per* RNA within ~1 h (37). The dead zone, where the network is insensitive to phase-shifting by light, can be accounted for by a strongly nonlinear phosphatase-kinase (*PH-S*) interaction. (*B*) *per* RNA shown for 50 clock neurons whose repressor and promoter feedback loops synchronize together in constant darkness through the exchange of VIP. Neurons are given a Gaussian distribution in the period lengths of their repressor and promoter feedback loops, with an average period of 24.0 h and a standard deviation of 1.2 h. (*C*) *Upper*: Synchronization order parameter, $synch = \frac{\text{variance}_{\text{time}}[\text{mean}_{\text{neuron i}}[MP_i]]}{\text{mean}_{\text{neuron i}}[\text{variance}_{\text{time}}[MP]_i]}$, where 1.0 is perfect synchronization and 0.0 is no synchronization (19,21). *Middle*: Scaled firing rate, *R*, which oscillates by an factor of ~2. *Lower*: Second-messenger MAPK *S*. (*D*) Phase response curve constructed by measuring the model network's phase shift due to a 15-min pulse of light in constant darkness (light pulse represented by $ptrbR = 0.04$ in Eq. A13 and $ptrbS = 0.08$ in Eq. A14).

tract, which terminates in the VL part of the SCN (2), where they increase the average firing rate, which in turn increases the rate at which VIP is transmitted between clock neurons. Both PACAP and VIP are known to bind to the $VPAC_2$ receptor, from which they initiate cAMP/PKA, Ca^{2+}, and MAP kinase signaling pathways that lead to the phosphorylation of cAMP response element binding protein (CREB), which in turn leads to the induction of *per* (38,43,44). However, it has been found recently that acute light-dependent increase of *per* RNA in mouse can result via an *n*-methyl-*d*-aspartate (NMDA) receptor pathway that is independent of VIP (45), so it appears that *per* transcription can be activated by both the VIP and NMDA pathways. Part of the mechanism involves a kinase being translocated to the nucleus, where it turns on CREB, a nuclear transcription factor that binds to a specific sequence of DNA to upregulate clock gene transcription. In the nucleus, phosphorylated CREB acts independently of the CLOCK-BMAL1 promoter to induce both *per* and *mkp1* transcription (46), so we assume that the VIP/NMDA→MAPK→CREB and CLOCK-BMAL1 pathways act in parallel to promote *per* transcription. It would seem that VIP is forcing a *per* oscillation in constant darkness and light-induced *per* is phase-shifting the oscillation.

Clock neurons are unusual in that they spike only slowly in the 1- to 10-Hz range. Their average firing rate oscillates in constant darkness, increasing by a factor of ~2 during subjective day, with their peak firing rate occurring around circadian time 7 (47), ~1 h before the peak in *per* RNA (37). Together, these findings lend support to the hypothesis that in constant darkness, an oscillation in the VIP should be able to drive both firing rate and *per* transcription so as to synchronize the network. Also, the hyperpolarizing neurotransmitter GABA is cotransmitted along with depolarizing VIP, and SCN neurons are ~3 times more likely to increase their firing rate during subjective night, when GABA cotransmission is lower, as compared with subjective day (48). We assume that one purpose of GABA cotransmission is to limit the increase in firing rate when a clock neuron receives VIP, so that during subjective day, when GABA exchange is relatively high, it causes the firing rate to saturate.

Central to the LG mammalian clock neuron model is the neuron's repressor feedback loop, where *per* and *cry* RNAs (*MP* and *MC*) are transcribed, translated into clock proteins (*PC* and *CC*), and then dimerized (*PCC*). As dimers they enter the nucleus to form a repressor that binds to CLOCK-BMAL1 promoter (*PCN* and *BN* dimerize to make *IN)*, thus inhibiting the transcription of *per* and *cry* RNA (24). Our model neuron's first 10 dimensions describe its repressor and promoter feedback loops and are taken directly from the LG model, from which we have omitted six phosphorylation-degradation pathways. We add six dimensions involving firing rate and VIP exchange between neurons so that each neuron is described by 16 variables shown in Fig. 2 *A*. Our model is a network of such neurons, each accounted for by 16 first-order differential equations, one each for the time rate of change of a neuron's *per*

RNA$\frac{dMP[t]}{dt}$, *cry* RNA$\frac{dMC[t]}{dt}$, etc. Below is a list of the variables, together with their interrelationships, that are accounted for by the time evolution of differential equations in the Appendix.

Repressor feedback loop:

1. *MP* = *per* RNA transcription activated by CLOCK-BMAL1 (*BN*), which is inhibited by nuclear PER-CRY dimer (*PCN*). This transcription is independently activated by phosphorylated CREB (*SN*).
2. *MC* = *cry* RNA transcription activated by CLOCK-BMAL1 (*BN*).
3. *PC* = PER protein translated from *per* RNA (*MP*).
4. *CC* = CRY protein translated from *cry* RNA (*MC*).
5. *PCC* = PER-CRY dimer made from *PC* and *CC*.
6. *PCN* = PER-CRY dimer in the nucleus, which binds CLOCK-BMAL1 (*BN*), repressing transcription of *per* and *cry*.

Promoter feedback loop:

7. *MB* = *bmal1* RNA, inhibited by nuclear BMAL1 (*BN*) protein. *clock* is transcribed at a constant rate so that its protein is considered an implicit part of BMAL1 (24).
8. *BC* = BMAL1 protein translated from *bmal1* RNA.
9. *BN* = nuclear BMAL1 protein, which inhibits *MB* and activates *per* and *cry* transcription.

Repressor loop couples to promoter loop:

10. *IN* = inhibitor of *per* and *cry* transcription. Inhibitor is made when PER-CRY (*PCN*) dimerizes to CLOCK-BMAL1 (*BN*), preventing it from activating *per* and *cry* transcription.

Negative feedback loop, in which received VIP damps a clock neuron's own VIP production:

11. *VP* = VIP precursor, inhibited by received VIP, presumably via nuclear CREB (*SN*).
12. *V* = VIP neuropeptide, made by VIP precursor and exchanged between clock neurons.
13. *R* = clock neuron firing rate.
14. *S* = MAP kinase phosphorylated due to VIP binding to the $VPAC_2$ receptor, as well as by NMDA receptors activated by afferents from ganglion cells exposed to light (45).
15. *SN* = nuclear CREB turned on by MAP kinase, which then induces *per* (*MP*) and *mkp1* (*PH*) transcription. We assume that *SN* damps VIP precursor (*VP*).
16. *PH* = MKP1 phosphatase whose RNA is induced by CREB (*SN*). *PH* dephosphorylates/shuts off the MAP kinase signal (*S*).

The repressor loop spontaneously oscillates in a limit cycle that depends on the strongly nonlinear feedback to RNA transcription provided by *BN* (see Appendix, Eqs. A1–A6). The promoter loop (*MB*, *BC*, and *BN* in Eqs. A7–A9) also oscillates, but this oscillation depends upon a weaker nonlinearity for its negative feedback than does the repressor loop and so has a smaller exponent—$m = 2$ in Eq. A7 versus $n = 4$ in Eqs. A1 and A2—and is less rhythmic than the repressor loop (24).

In constant darkness, the SCN is able to compromise on a free-running period (FRP) that varies from animal to animal but is usually within a half-hour of 24 h long (1,2). However, single neurons within the SCN have a wide variance in the natural period of their repressor and promoter feedback loops, with period lengths that range between 22 and 28 h (1). To obtain a distribution of natural periods within the network, we used a Gaussian-distributed random variable, s_i, as a scale factor that multiplied all the rate constants for the repressor and promoter feedback loops inside a given neuron ($s_i = 1.0 \pm 0.05$ standard deviation in Eqs. A1–A10) We did not include such rate-constant noise in the VIP feedback loop, although small amounts of it produced similar results (include scale factor with 0.02 standard deviation in Eqs. A11–A16). Also, although the VL SCN includes several thousand neurons, we were only able to simulate all-to-all coupling between 50 neurons for times <1000 h on a PC. Simulations were run using Mathematica 5.2 on a Dell computer with a Microsoft Windows XP operating system and an Intel Pentium 4 processor (model in support file). We construct a basic model in which light causes a fast increase in second messenger (*S*), which induces both *per* and phosphatase transcription. Induced *per* phase-shifts the repressor feedback loops inside the clock neurons, whereas high levels of phosphatase block further second-messenger signal and establish a dead zone in which the clock neurons become insensitive to phase-shifting by light.

SIMULATION RESULTS

A network of LG model clock neurons can be coupled together through the exchange of the neuropeptide VIP. When VIP is made to oscillate in a 12-h negative feedback loop (*VP*, *V*, *R*, *S*, *SN*; Eqs. A11–A15) received VIP causes fast *per* transcription, which synchronizes all the repressor loops together in constant darkness (Eq. 1 and Fig. 2 *B*). This synchronization depended on several factors: first, that the received neuropeptide would quickly increase firing rate together with *per* transcription; second, that the received neuropeptide would slowly couple back to inhibit the neuropeptide precursor; and third, that this feedback loop would be strongly rhythmic. Strong rhythmicity in turn depended on the received VIP inhibiting a clock neuron's own VIP production through a high-gain, nonlinear negative feedback (Eq. A11).

Electrically we consider a clock neuron as a small capacitor with a voltage threshold that, when surpassed, results in an action potential. A VIP received from other clock neurons increases membrane potential and firing rate, whereas a received GABA has the opposite effect, decreasing membrane potential and firing rate. Firing rate is also increased by positive leak conductance turned on by retinal ganglion cells that are exposed to light. Thus, our target

firing rate is proportional to the product of the average firing rate and the VIP $\overline{(R \times V)}$ when this product is small, but then saturates due to the cotransmission of GABA when this product becomes large. In addition, the target firing rate includes a step function representing input from retinal ganglion cells that are exposed to light (Eqs. A13 and A13a).

We obtained a phase-response curve (PRC) for the synchronized network where a pulse of light was represented by two step functions that immediately increased the rates of change of both the firing rate and the second messenger. Then, by adjusting the strength of these light-induced increases in $\dot{R}$ and $\dot{S}$, the recorded phase shifts due to 15-min light pulses could be made similar to PRCs obtained from mammalian experiments (2,52) (Fig. 2 *D*). Physically, light causes the transmission of glutamate and PACAP along axons of the retino hypothalamic tract to the VL SCN, so it is logical that the light-induced second messenger (S) exists in part due to PACAP binding to the $VPAC_2$ receptor (53). Also, it is now known that acute light-dependent increase of *per* RNA in mouse can result via an NMDA receptor pathway that is independent of VIP and the $VPAC_2$ receptor (45). Meanwhile, VIP (V) is being continuously exchanged between clock neurons, so our second-messenger target was proportional to the product of the average firing rate and the VIP $\overline{(R \times V)}$ plus a step that we attribute to light-induced input from retinal ganglion cells (Eqs. A14 and A14a). Light-induced increases in firing rate also act to increase S.

The generic PRC includes an interesting region ~9 h long called the dead zone, where the mammal is insensitive to phase-shifting by light (2). Unlike the mammal, fruit fly clock neurons see the light, which acts directly through chromophores within them to degrade clock proteins and induce phase shifts (54). Clock protein concentration oscillates so that when it is low, the fly becomes insensitive to phase shifting by light. However, it appears that phase-shifting and dead zone in mammals work by a different principle, since mammalian clock neurons are kept from seeing sunlight directly and their clock proteins are known to peak during the late part of the dead zone. In the mammal, instead of degrading clock proteins, light induces transcription of both *per* and *mkp1* phosphatase (37,38). It is interesting that light uses cAMP/PKA, Ca^{2+}, and MAP kinase signaling pathways for this gene induction and that one of the induction targets is a phosphatase that dephosphorylates MAP kinase. This interaction between kinase and phosphatase is known to be very strongly nonlinear, and we hypothesize that it is responsible for the dead zone ((55); exponent $q = 50$ step function in Eq. 14b). Light causes an increase in phosphorylated kinase signal, which is followed by the induction of dephosphorylated phosphatase. Kinase phosphorylates the phosphatase, changing its conformation so that it will dephosphorylate a future kinase signal (55). Thus, whenever the kinase-phosphatase product exceeds a certain threshold, it will establish a dead zone. This interaction acts to truncate the phosphorylated kinase signal (Fig. 2 *C*), and effectively would make the SCN into a light-edge detector.

In constant darkness, our simulated dead zone is generic and ~9 h long (2). Note that there is experimental evidence that the width of the Siberian hamster's dead zone shortens to ~7 h after the animal has been entrained to a winter 9-15 light-dark cycle (52), the implication being that cycle memory makes the dead zone into a dynamic rather than a static interval. We note that in our simulations, the dead zone expands to ~12 h after entrainment to a summer 16-8 light-dark cycle. However, our simulated dead zone does not shorten after entrainment to a winter 8-16 cycle, but would do so if short day lengths were to downregulate VIP to second-messenger signaling $\overline{(R \times V)} \rightarrow S$. Also, there is recent experimental evidence that something like a kinase-phosphatase mechanism is responsible for the dead zone. Without $VPAC_2$ signaling, the mouse SCN becomes inappropriately responsive to phase shifting by light during the day, the implication being that VIP signaling is responsible for the dead zone, as shown by Maywood et al. (45). In that experiment, light via an NMDA pathway was able to acutely induce *per* during the supposed dead zone for the $Vipr2^{-/-}$ mutant mouse whose *mPer1* RNA (and presumably also *mkp1* RNA) remained low throughout the circadian day. In our model, it is VIP-driven *mkp1* induction that is responsible for the dead zone.

We tested the model's ability to entrain to the circadian day by using step functions to make sequences of light periods. The network had a free-running period of 24.0 h and was able to phase shift by 10–12 h in 6–7 days, advancing or delaying to acquire lock to a 12-12 light-dark cycle (Fig. 3). Increasing or decreasing the coupling strength between light and the network respectively decreased or increased the time to acquire the cycle. The coupling strengths, $ptrbR = 0.006$ in Eq. A13 and $ptrbS = 0.006$ in Eq. A14, were chosen to be consistent with time-to-entrain, cycle-memory, and limits-of-entrainment experiments ((1); see Fig. 1 *B*).

We next investigated the model's memory for the particular light-dark cycle to which it was entrained, together with its limits of entrainment. Fireflies are known to have a resetting strength where a larger strength permits synchronization between two flies with more dissimilar frequencies (49–51). Here, the coupling is between a network with a 24.0-h free-running period and a specific light-dark cycle. Our light periods are defined by the height of the step changes they make in $\dot{R}$ and $\dot{S}$ ($ptrbR = 0.006$ in Eq. A13 and $ptrbS = 0.006$ in Eq. A14). This choice permitted the network to entrain cycle lengths between ~22 and 26 h, whereas our experimental range of entrainment was 20–26 h (Fig. 4, *A*, *B*, *E*, and *F*). Holding day length constant, we locked the network to various light-dark cycles. When fixed to a 24-h day length, the model was able to remember the particular cycle, i.e., 10-14, 14-10, etc. that it was locked to as it proceeded into constant darkness (Fig. 4, *C* and *D*). Cycle-rate memory tests began with 12-12 light-dark cycles, which for 12 days increased or decreased their light period by 10 min per day to mimic large day-length changes that occur at

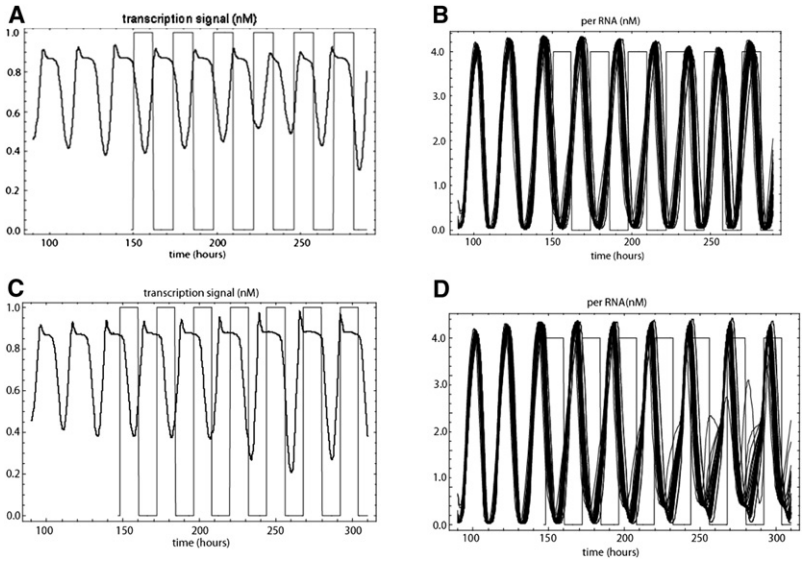

FIGURE 3 Entrainment of the model network to a sequence of 12-12 light-dark cycles. (*A* and *B*) It takes ~6 days to phase-advance by ~12 h to entrain the transcription signal (*SN*) (*A*) and *per* RNA (*MP*) (*B*). (*C* and *D*) It takes ~7 days for a 10-h phase delay to entrain the transcription signal (*C*) and *per* RNA (*D*). Light periods are shown as sequences of black rectangles and represented by $ptrbR = 0.006$ in Eq. A13 and $ptrbS = 0.006$ in Eq. A14.

high latitudes near an equinox (56). Again, similar to our experimental animals, the model was able to anticipate the expected light and dark edges as it proceeded into constant darkness (Fig. 4, *G* and *H*).

We next reduced the rythmicity of the VIP feedback loop, and this resulted in an immediate large phase shift as the model proceeded into constant darkness, which we interpreted as a loss of cycle memory (Fig. 4 *I*). We tested the opposite effect, reducing the effect of light on a strongly rhythmic VIP oscillation, which markedly increased the duration of cycle memory (Fig. 4 *J*). Thus, it appears that light-dark cycle memory and cycle-rate memory can be accounted for by a strongly rhythmic neuropeptide feedback loop upon which light acts as a perturbation. For memory, what is important is that the light-perturbed VIP limit cycle be similar to the unperturbed cycle. Note that the SCN is ~100 times less sensitive to light than are the retina's rod cells (48). Note also that increasing the coupling strength between light and the SCN will increase the range of entrainment and shorten the acquisition time, but that these changes come at the expense of cycle memory.

DISCUSSION

A strongly nonlinear negative feedback appears to be required to maintain the limit-cycle oscillation in the biochemistry inside an individual clock neuron (24). Leloup and Goldbeter noted that the strong rhythmicity within a clock neuron's repressor feedback loop depended upon a strongly nonlinear negative feedback, characterized by a nonlinear feedback equation that used an exponent significantly greater than 1 ($n = 4$ in Eqs. A1 and A2). This choice made for a robust circadian oscillation of the clock proteins PER and CRY within a single uncoupled clock neuron in constant darkness. Apparently, strong nonlinearities are also required in the coupling pathway between clock neurons to compete against and overcome the cell's own natural rhythm, so as to be able to synchronize clock neurons in constant darkness. Strong nonlinearity within the neuropeptide feedback loop in the synchronization pathway between clock neurons allows for a high-contrast synchronizing signal to be exchanged between them, which then leads to a high degree of synchronization (exponents o in Eq. A1 and p in Eq. A11). Also, a strongly rhythmic VIP oscillation on which light acts only weakly leads functionally to light-dark cycle memory. This can be obtained by making the negative feedback within the loop strongly nonlinear (exponent $p = 4$ in Eq. A11) and also by increasing loop gain (*c4* in Eq. A11, *c9* in Eq. A13a, and *c11* in Eq. A14a).

There is some controversy concerning the intrinsic rhythmicity of clock neurons, whether many remain rhythmic when uncoupled, and whether coupling should convey both synchronicity and rhythmicity upon them (3,23). Indeed, if a particular clock neuron has strong intrinsic rhythmicity with a period length that is several hours distinct from the circadian day then it would seem that a very strong coupling would be required to synchronize it to the day. It is evident that a natural competition should arise between the intrinsic rhythmicity of an individual clock neuron and the rhythmicity of the loop that synchronizes them together. It is possible that many repressor and promoter feedback loops are intentionally made only weakly rhythmic to permit easier synchronization between them.

There is a natural question concerning the multiple actions of the VIP: why should VIPs act quickly to increase firing rate while at the same time inducing clock gene transcription and then later inhibit a clock neuron's own VIP production? Compare the VIP oscillation in the SCN in complete darkness with the voltage oscillation in a hair cell in the frog's hearing organ in complete quiet (57). In the quiet, a current of potassium ions leaks into the hair cell, which depolarizes it and turns on a fast, voltage-gated calcium current that further depolarizes

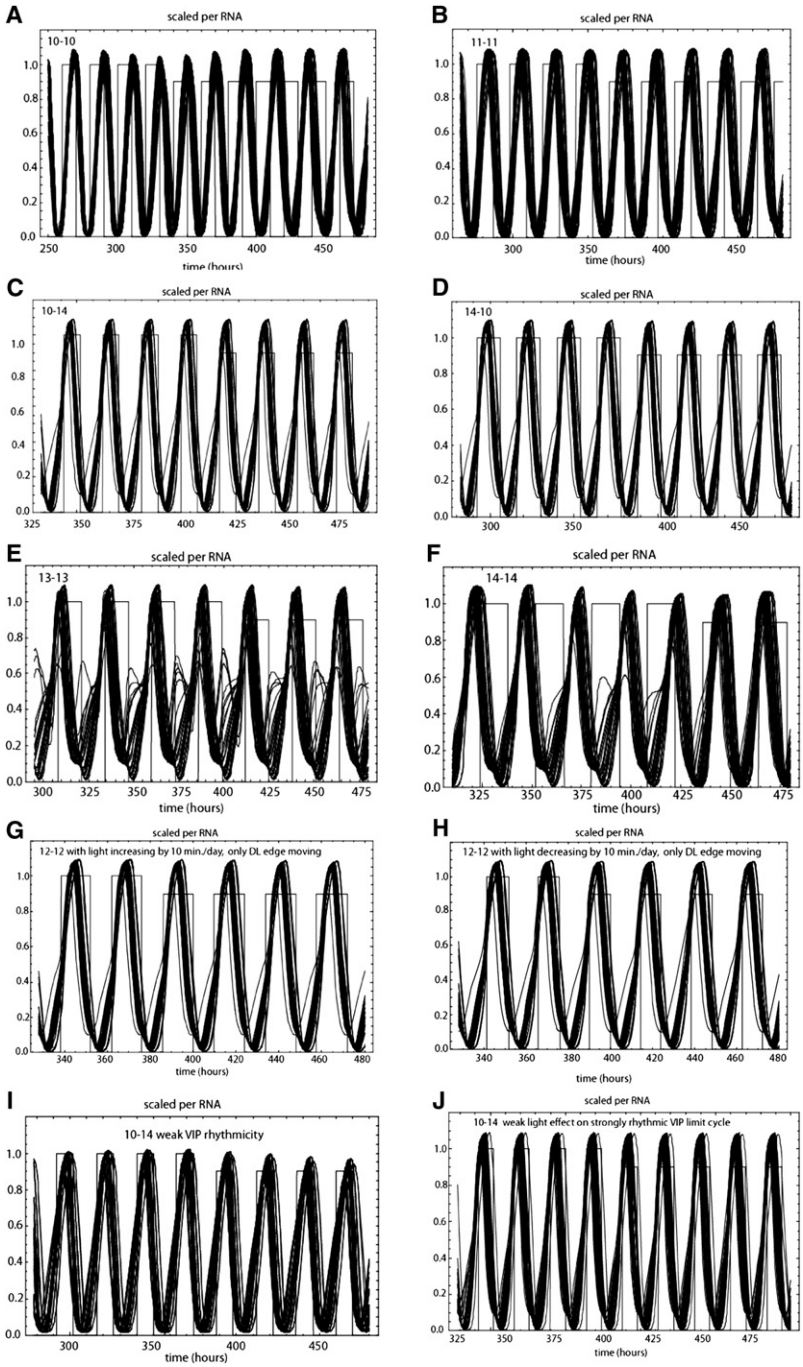

FIGURE 4 Light-dark cycle memory and range of entrainment. *per* RNA (*MP*) is shown for the last several of 12 days of light-dark cycles. Periods of light are indicated by the tall rectangles, whereas the shorter rectangles are in constant darkness and show where the light would be if the cycle were continued. Network phase shifts (PS) for the first several days in constant darkness can be seen by eye, but in the caption we give PS1, 2 and 3 for the first, second and third days in constant darkness with respect to the last day on the light-dark cycle. (*A*) Model with an FRP of 24.0 h was unable to lock a 10-10 cycle. (*B*) The same model as in *A* was able to lock an 11-11 cycle (PS1 = 0, PS2 = −119 min., and PS3 = −200 min). (*C*) Model with a 10-14 cycle had 1 day of memory before the phase advance (PS1 = 0, PS2 = +13 min., and PS3 = +13 min). (*D*) Model with a 14-10 cycle had 1 day of memory before phase delay (PS1 = 0, PS2 = −47 min., and PS3 = −47 min). (*E*) Model with a 13-13 cycle had 1 day of memory before phase advance (PS1 = 0, PS2 = +30 min, and PS3 = +54 min). (*F*) Model was unable to lock a 14-14 cycle. (*G*) Model with a 12-12 cycle whose light was advanced/increased by 10 min/day shows ~1 day of cycle-rate memory before phase delay (PS1 = 0, PS2 = −32 min, and PS3 = −47 min). (*H*) Model with a 12-12 cycle whose light period was delayed/decreased by 10 min/day also had 1 day of cycle-rate memory before phase advance (PS1 = 0, PS2 = +32 min, and PS3 = +32 min). (*I*) Memory lost for a 10-14 cycle when rhythmicity of the VIP oscillation was reduced (*c4* 0.37 → 0.36 in Eq. A11; *c9* 1.5 → 1.45 in Eq. A13a; *c11* 2.0 → 1.5 in Eq. A14a; *s* 0.96 → 0.88 to maintain 24.0-h period; PS1 = −15 min., PS2 = −146 min., PS3 = −176 min). (*J*) Duration of cycle memory markedly increased when the effect of light perturbation was decreased (*ptrbR* 0.006 → 0.002 in Eq. A13 and *ptrbS* 0.006 → 0.002 in Eq. A14; PS1 = PS2 = PS3 = 0). It is evident that cycle memory depends on light acting as a small perturbation on a strongly rhythmic underlying limit cycle.

it (fast positive feedback). Calcium then binds with a time delay to a calcium-gated potassium channel, which hyperpolarizes the cell (time-delayed negative feedback). When hyperpolarized, all channels turn off and the leak current then restarts the cycle so that hair cell voltage sinusoidally oscillates by several millivolts in the quiet. Note that if the calcium current were not providing fast positive feedback, the hair cell would not oscillate. Compare this to the neuropeptide oscillation in the SCN in constant darkness: as transmitted VIP increases, the firing rate increases, which then further increases transmitted VIP (fast positive feedback). The received VIP then inhibits VIP production with a time delay (time-delayed negative feedback). Similar to turning off the calcium current in the hair cell, if one reduces the VIP to firing-rate gain then the VIP oscillation can be turned off. In both cases, a fast positive feedback followed by a slow negative one makes for spontaneous oscillation in the quiet or in the dark.

Day length on earth is almost exactly 24 h, with the only change being that hours of light are continually being traded for hours of darkness as we go from summer to winter, and vice versa. At 45° north latitude, our light-dark period changes from 16-8 in the summer to 9-15 in the winter, with

the fastest rate of decrease in light occurring near the fall equinox, where the light period is shortening by ~4 min/day (56). What is the advantage to mammalian life on a rotating world that it be able to remember the light-dark cycle and the rate of change of this light-dark cycle? The SCN is in effect remembering the entraining signal by persisting with a long-lived transient limit cycle in its synchronized repressor feedback loops inside its coupled clock neurons. Here, a comparison to electronics is useful: a second-order lock-in amplifier creates a replica signal at a slowly moving entraining frequency and thereby forms a memory for that entraining signal (58). Then, its replica remains close to its locked frequency in the event of a signal dropout, so that when the signal returns, reacquisition by lock-in or pull-in is very rapid. In a lock-in amplifier, an active high-gain feedback loop is responsible for the long holding times. Also note that a third-order lock-in has frequency-rate memory together with frequency and phase memories. Thus, it appears that it is possible to make a reasonable comparison between the mammalian SCN, with its high-gain VIP feedback loop, and a high loop-gain lock-in amplifier. Here, rapid signal reacquisition in case of a light-dark cycle dropout would seem to be one clear advantage. A second advantage for precisely remembering the location of the light and dark edges would likely be light-noise rejection, so that spurious or unexpected light or dark edges would result in minimal phase shifts. Here, we note that the mammalian SCN has a type 1 PRC with a dead zone that rejects light-noise during the day, unlike simpler life forms with type 0 PRCs that lack a dead zone and thus permit light to phase-shift the organism throughout the day (1). Investigations need to be made into the noise-rejection properties of a type 1 PRC with a dynamic dead zone.

We have shown that Siberian hamsters have several days of memory for a light-dark cycle. Cycle memory appears to be due to a strongly rhythmic VIP oscillation and the dead zone in mammals can result from a strongly nonlinear kinase-phosphatase interaction. A good SCN is an extremely accurate timepiece that is correct to within several minutes out of the 1440 in a day (3). In the way that its clock neurons are intentionally kept in the dark and isolated from spurious light, as well as the way that the biochemical limit cycles of its clock neurons form a replica of a light-dark cycle, and thus retain a memory of the entraining light-dark signal, the mammalian SCN resembles a lock-in amplifier (58).

APPENDIX

A clock neuron is represented by 16 dynamical variables: MP, MC, PC, CC, PCC, PCN, MB, BC, BN, IN, VP, V, R, S, SN, and PH. The first 10 are taken directly from the LG mammalian clock neuron model (24). Below is a list of the 16 differential equations together with three auxiliary equations that represent one clock neuron. The parameters and Mathematica model can be found in the Supporting Material. s is a scale factor that sets the average natural period of the clock neurons, and the random variable s_i scales a particular neuron's repressor and promoter feedback loops to vary this period.

Repressor feedback loop

$$\frac{dMP[t]}{dt} = s\ s_i\left(vsP\ \frac{BN[t]^n}{KAP^n + BN[t]^n} + c1\frac{SN[t]^o}{c2^o + SN[t]^o} - vmP\frac{MP[t]}{KmP + MP[t]} - kdmp\ MP[t]\right) \tag{A1}$$

$$\frac{dMC[t]}{dt} = s\ s_i\left(vsC\frac{BN[t]^n}{KAC^n + BN[t]^n} - vmC\frac{MC[t]}{KmC + MC[t]} - kdmc\ MC[t]\right) \tag{A2}$$

$$\frac{dPC[t]}{dt} = s\ s_i\left(ksP\ MP[t] + k4\ PCC[t] - v1P \times\frac{PC[t]}{Kp + PC[t]} - k3\ PC[t]\ CC[t] - kdpc\ PC[t]\right) \tag{A3}$$

$$\frac{dCC[t]}{dt} = s\ s_i\left(ksC\ MC[t] + k4\ PCC[t] - v1C \times\frac{CC[t]}{Kp + CC[t]} - k3\ PC[t]\ CC[t] - kdcc\ CC[t]\right) \tag{A4}$$

$$\frac{dPCC[t]}{dt} = s\ s_i\left(k3\ PC[t]\ CC[t] + k2\ PCN[t] - V1PC\ \frac{PCC[t]}{Kp + PCC[t]} - k4\ PCC[t] - k1\ PCC[t] - kdpcc\ PCC[t]\right) \tag{A5}$$

$$\frac{dPCN[t]}{dt} = s\ s_i\left(k1\ PCC[t] + k8\ IN[t] - V3PC\ \frac{PCN[t]}{Kp + PCN[t]} - k2\ PCN[t] - k7\ BN[t]\ PCN[t] - kdpcn\ PCN[t]\right) \tag{A6}$$

Promoter feedback loop

$$\frac{dMB[t]}{dt} = s\ s_i\left(vsB\ \frac{KIB^m}{KIB^m + BN[t]^m} - vmB \times\frac{MB[t]}{KmB + MB[t]} - kdmb\ MB[t]\right) \tag{A7}$$

$$\frac{dBC[t]}{dt} = s\ s_i\Big(ksB\ \ MB[t] + k6\ \ BN[t] - V1B\frac{BC[t]}{Kp\ \ + BC[t]} - k5\ \ BC[t]\ \ - kdbc\ \ BC[t]\Big) \tag{A8}$$

$$\frac{dBN[t]}{dt} = s\ s_i\Big(k5\ \ BC[t]\ + k8\ \ IN[t] - V3B\frac{BN[t]}{Kp\ \ + BN[t]} - k6\ \ BN[t]\ \ - k7\ \ BN[t]\ \ PCN[t] - kdbn\ \ BN[t]\Big) \tag{A9}$$

Coupling between repressor and promoter feedback loops

$$\frac{dIN[t]}{dt} = s\ s_i\Big(k7\ \ BN[t]\ \ PCN[t] - k8\ \ IN[t] - vdIN\frac{IN[t]}{Kd\ \ + IN[t]} - kdi\ \ IN[t]\Big) \tag{A10}$$

VIP feedback loop

$$\frac{dVP[t]}{dt} = s\ \left(c3 - c4\ \frac{SN[t]^p}{c5^p\ \ + SN[t]^p} - c6\ \ VP[t]\right) \tag{A11}$$

$$\frac{dV[t]}{dt} = s\ \left(\frac{VP[t] - V[t]}{tv}\right) \tag{A12}$$

$$\frac{dR[t]}{dt} = s\ \left(\frac{Rinf[t]\ + ptrbR\ \ \ UnitStep[t - ptrbt]\ \ \ UnitStep[ptrbt\ + step - t] - R[t]}{tR}\right) \tag{A13}$$

$$Rinf[t] = c8\ + c9\ \frac{\Sigma_{j=1}^{NN}\ \left(R_j[t]\ \ V_j[t]\right)}{NN} - c10\ \frac{\Sigma_{j=1}^{NN}\ \left(R_j[t]\ \ V_j[t]\right)^2}{NN} \tag{A13a}$$

$$\frac{dS[t]}{dt} = s\ \left(\frac{Sinf[t]\ + ptrbS\ \ \ UnitStep[t - ptrbt]\ \ \ UnitStep[ptrbt\ + step - t] - DZ[t] - S[t]}{tS}\right) \tag{A14}$$

$$Sinf[t] = c11\ \frac{\Sigma_{j=1}^{NN}\ \left(R_j[t]\ \ V_j[t]\right)}{NN} \tag{A14a}$$

$$DZ[t] = \frac{(S[t]\ \ PH[t])^q}{c7^q\ + (S[t]\ \ PH[t])^q} \tag{A14b}$$

$$\frac{dSN[t]}{dt} = s\ \left(\frac{S[t] - SN[t]}{tSN}\right) \tag{A15}$$

Phosphatase

$$\frac{dPH[t]}{dt} = s\left(\frac{SN[t] - PH[t]}{tPH}\right) \tag{A16}$$

SUPPORTING MATERIAL

The Mathematica model of the ventrolateral SCN is available at http://www.biophysj.org/biophysj/supplemental/S0006-3495(09)01114-X.

We thank the animal care staff at the University of Memphis, and Shing Lam for compiling the C code based on a formula first published by Meeus (56).

Funds were provided by the University of Memphis.

REFERENCES

1. Dunlap, J. C., J. J. Loros, and P. J. Decoursey. 2004. Chronobiology: Biological Timekeeping. Sinauer, Sunderland, MA.
2. Moore, R. Y. 1999. Circadian timing. *In* Fundamental Neuroscience. Michael J. Zigmond, Floyd E. Bloom, Story C. Landis, James L. Roberts, and Larry R. Squire, editors. Academic Press, San Diego, CA. 1198–1206.
3. Aton, S. J., and E. D. Herzog. 2005. Come together, right…now: synchronization of rythms in a mammalian circadian clock. *Neuron*. 48:531–534.
4. Reppert, S. M., and D. R. Weaver. 2002. Coordination of circadian timing in mammals. *Nature*. 418:935–941.
5. Stephan, F. K., and I. Zucker. 1972. Circadian rhythms in drinking behavior and locomotor activity of rats are eliminated by hypothalamic lesions. *Proc. Natl. Acad. Sci. USA*. 69:1583–1586.
6. Welsh, D. K., D. E. Logothetis, M. Meister, and S. M. Reppert. 1995. Individual neurons dissociated from rat superchiasmatic nucleus express independently phased circadian firing rhythms. *Neuron*. 14:697–706.
7. Abrahamson, E. E., and R. Y. Moore. 2001. Suprachiasmatic nucleus in the mouse: retinal innervation, intrinsic organization and efferent projections. *Brain Res*. 916:172–191.
8. Aton, S. J., C. S. Colwell, A. J. Hammar, J. Waschek, and E. D. Herzog. 2005. Vasoactive intestinal polypeptide mediates circadian rhythmicity and synchrony in mammalian clock neurons. *Nat. Neurosci*. 8:476–483.
9. Brown, T. M., A. T. Hughes, and H. D. Piggins. 2005. Gastrin-releasing peptide promotes suprachiasmatic nuclei cellular rhythmicity in the absence of vasoactive intestinal polypeptide-VPAC2 receptor signaling. *J. Neurosci*. 25:11155–11164.
10. Liu, C., and S. M. Reppert. 2000. GABA synchronizes clock cells within the suprachiasmatic circadian clock. *Neuron*. 25:123–128.

11. Maywood, E. S., A. B. Reddy, G. K. Wong, J. S. O'Neill, J. A. O'Brien, et al. 2006. Synchronization and maintenance of timekeeping in suprachiasmatic circadian clock cells by neuropeptidergic signaling. *Curr. Biol.* 16:599–605.
12. Piggins, H. D., M. C. Antle, and B. Rusak. 1995. Neuropeptides phase shift the mammalian circadian pacemaker. *J. Neurosci.* 15:5612–5622.
13. Reed, H. E., A. Meyer-Spasche, D. J. Cutler, C. W. Coen, and H. D. Piggins. 2001. Vasoactive intestinal polypeptide (VIP) phase-shifts the rat suprachiasmatic nucleus clock in vitro. *Eur. J. Neurosci.* 13:839–843.
14. Shen, S., C. Spratt, W. J. Sheward, I. Kallo, K. West, et al. 2000. Overexpression of the human VPAC2 receptor in the suprachiasmatic nucleus alters the circadian phenotype of mice. *Proc. Natl. Acad. Sci. USA.* 97:11575–11580.
15. Harmar, A. J., H. M. Marston, S. Shen, C. Spratt, K. M. West, et al. 2002. The VPAC(2) receptor is essential for circadian function in the mouse suprachiasmatic nuclei. *Cell.* 109:497–508.
16. Itri, J., and C. S. Colwell. 2003. Regulation of inhibitory synaptic transmission by vasoactive intestinal peptide (VIP) in the mouse suprachiasmatic nucleus. *J. Neurophysiol.* 90:1589–1597.
17. Aton, S. J., J. E. Huettner, M. Straume, and E. D. Herzog. 2006. GABA and $G_{i/o}$ differentially control circadian rhythms and synchrony in clock neurons. *Proc. Natl. Acad. Sci. USA.* 103:19188–19193.
18. Strogatz, S. 1987. Human sleep and circadian rythms: a simple model based on two coupled oscillators. *J. Math. Biol.* 25:327–347.
19. Garcia-Ojalvo, J., M. B. Elowitz, and S. H. Strogatz. 2004. Modeling a synthetic multicellular clock: repressilators coupled by quorum sensing. *Proc. Natl. Acad. Sci. USA.* 101:10955–10960.
20. Antle, M. C., D. K. Foley, N. C. Foley, and R. Silver. 2003. Gates and oscillators: a network model of the brain clock. *J. Biol. Rhythms.* 18:339–350.
21. Gonze, D., S. Bernard, C. Waltermann, A. Kramer, and H. Herzel. 2005. Spontaneous synchronization of coupled circadian oscillators. *Biophys. J.* 89:120–129.
22. Bernard, S., D. Gonze, B. Cajavec, H. Herzel, and A. Kramer. 2007. Synchronization-induced rythmicity of circadian oscillators in the superchiasmatic nucleus. *PLOS Comput. Biol.* 3:667–679.
23. To, T.-L., M. A. Hensen, E. D. Herzog, and F. J. Doyle, III. 2007. A molecular model for intercellular synchronization in the mammalian circadian clock. *Biophys. J.* 92:3792–3803.
24. Leloup, J.-C., and A. Goldbeter. 2003. Toward a detailed computational model for the mammalian circadian clock. *Proc. Natl. Acad. Sci. USA.* 100:7051–7056.
25. Forger, D. B., and C. S. Peskin. 2003. A detailed predictive model of the mammalian circadian clock. *Proc. Natl. Acad. Sci. USA.* 100:14806–14811.
26. Forger, D. B., and C. S. Peskin. 2005. Stochastic simulation of the mammalian circadian clock. *Proc. Natl. Acad. Sci. USA.* 102:321–324.
27. Leloup, J.-C., and A. Goldbeter. 2004. Modeling the mammalian circadian clock: sensitivity analysis and multiplicity of oscillatory mechanisms. *J. Theor. Biol.* 230:541–562.
28. Hao, H., D. E. Zak, T. Sauter, J. Schwaber, and B. A. Ogunnaike. 2006. Modeling the $VPAC_2$-activated cAMP/PKA signaling pathway: from receptor to circadian clock gene induction. *Biophys. J.* 90:1560–1571.
29. Forger, D. B., D. Gonze, D. Virshup, and D. K. Welsh. 2007. Beyond intuitive modeling: combining biophysical models with innovative experiments to move the circadian clock field forward. *J. Biol. Rhythms.* 22:200–210.
30. Indic, P., W. J. Schwartz, E. D. Herzog, N. C. Foley, and M. C. Antle. 2007. Modeling the behavior of coupled cellular circadian oscillators in the superchiasmatic nucleus. *J. Biol. Rhythms.* 22:211–219.
31. Yamaguchi, S., H. Isejima, T. Matsuo, R. Okura, K. Yagita, et al. 2003. Synchronization of cellular clocks in the suprachiasmatic nucleus. *Science.* 302:1408–1412.
32. Shinohara, K., S. Honma, Y. Katsuno, H. Abe, and K. Honma. 1995. Two distinct oscillators in the rat suprachiasmatic nucleus. *Proc. Natl. Acad. Sci. USA.* 92:7396–7400.
33. Yin, L., J. Wang, P. S. Klein, and M. A. Lazar. 2006. Nuclear receptor Rev-erbα is a critical lithium-sensitive component of the circadian clock. *Science.* 311:1002–1005.
34. Harada, Y., M. Sakai, N. Kurabayashi, T. Hirota, and Y. Fukada. 2005. Ser-557-phosphorylated mCRY2 is degraded upon synergystic phosphorylation by glycogen synthase kinase-3β. *J. Biol. Chem.* 280:31714–31721.
35. Iitaka, C., K. Miyazaki, T. Akaike, and N. Ishida. 2005. A role for glycogen synthase kinase-3β in the mammalian circadian clock. *J. Biol. Chem.* 280:29397–29402.
36. Shinohara, K., K. Tominaga, Y. Isobe, and S.-I. T. Inouye. 1993. Photic regulation of peptides located in the ventrolateral subdivision of the suprachiasmatic nucleus of the rat: daily variations of vasoactive intestinal polypeptide, gastrin-releasing peptide, and neuropeptide Y. *J. Neurosci.* 13:793–800.
37. Zylka, M. J., L. P. Shearman, D. R. Weaver, and S. M. Reppert. 1998. Three period homologs in mammals: differential light responses in the suprachiasmatic circadian clock and oscillating transcripts outside of the brain. *Neuron.* 20:1103–1110.
38. Doi, M., S. Cho, I. Yujnovsky, J. Hirayama, N. Cermakian, et al. 2007. Light-inducible and clock-controlled expression of MAP kinase phosphatase 1 in mouse central pacemaker neurons. *J. Biol. Rhythms.* 22: 127–139.
39. Reference deleted in proof.
40. Pakhotin, P., A. J. Harmar, A. Verkhratsky, and H. Piggins. 2006. VIP receptors control excitability of suprachiasmatic nuclei neurons. *Eur. J. Phys.* 452:7–15.
41. Pennartz, C. M. A., M. T. G. De Jeu, N. P. A. Bos, J. Schaap, and A. M. S. Geurtsen. 2002. Diurnal modulation of pacemaker potentials and calcium current in the mammalian circadian clock. *Nature.* 416:286–290.
42. Ikeda, M., T. Sugiyama, C. S. Wallace, H. S. Gompf, T. Yoshioka, et al. 2003. Circadian dynamics of cytosolic and nuclear Ca^{++} in single suprachiasmatic nucleus neurons. *Neuron.* 38:253–263.
43. Pizzio, G. A., E. C. Hainich, G. A. Ferreyra, O. A. Coso, and D. A. Golombek. 2003. Circadian and photic regulation of ERK, JNK and p38 in the hamster SCN. *Neuroreport.* 14:1417–1419.
44. Vosko, A. M., A. Schroeder, D. H. Loh, and C. S. Colwell. 2007. Vasoactive intestinal peptide and the mammalian circadian system. *Gen. Comp. Endocrinol.* 152:165–175.
45. Maywood, E., J. O'Neill, J. E. Chesham, and M. H. Hastings. 2007. Minireview: the circadian clockwork of the suprachiasmatic nuclei: analysis of a cellular oscillator that drives endocrine rhythms. *Endocrinology.* 148:5624–5634.
46. Travnickova-Bendova, Z., N. Cermakian, S. M. Reppert, and P. Sassone-Corsi. 2002. Bimodal regulation of mPeriod promoters by CREB-dependent signaling and CLOCK/BMAL1 activity. *Proc. Natl. Acad. Sci. USA.* 99:7728–7733.
47. Meijer, J. H., K. Watanabe, J. Schaap, H. Albus, and L. Detari. 1998. Light responsiveness of the suprachiasmatic nucleus: long-term multiunit and single-unit recordings in freely moving rats. *J. Neurosci.* 18:9078–9087.
48. Nakamura, T. J., K. Fujimura, S. Ebihara, and K. Shinohara. 2004. Light response of the neuronal firing activity in the suprachiasmatic nucleus of mice. *Neurosci. Lett.* 371:244–248.
49. Strogatz, S. 1994. Nonlinear Dynamics and Chaos. Perseus Books, Reading, MA.
50. Buck, J. 1988. Synchronous rhythmic flashing of fire flies, part II.*Q. Rev. Biol.* 63:265–289.
51. Strogatz, S. 2003. Sync: How Order Emerges from Chaos in the Universe, Nature, and Daily Life. Hyperion Press, New York.

52. Puchalski, W., and G. R. Lynch. 1992. Relationship between phase resetting and the free-running period in Djungarian hamsters. *J. Biol. Rhythms*. 7:75–83.

53. Colwell, C. S., S. Michel, J. Itri, W. Rodriguez, J. Tam, et al. 2004. Selective deficits in the circadian light response in mice lacking PACAP. *Am. J. Physiol.* 287:R1194–R1201.

54. Leloup, J.-C., and A. Goldbeter. 1998. A model for circadian rhythms in *Drosophila* incorporating the formation of a complex between the PER and TIM proteins. *J. Biol. Rhythms*. 13:70–87.

55. Theodosiou, A., and A. Ashworth. 2002. MAP kinase phosphatases. *Genome Biol.* 3 Reviews3009:1–10.

56. Meeus, Jean. 1991. Astronomical Algorithms. Willmann-Bell, Richmond, VA.

57. Ospeck, M., V. M. Eguíluz, and M. O. Magnasco. 2001. Evidence of a Hopf bifurcation in frog hair cells. *Biophys. J.* 80:2597–2607.

58. Gardner, F. M. 1979. Phaselock Techniques,2nd ed . John Wiley and Sons, New York.